01 Jan 1988

Oxygen Tension Profiles In Tumors Predicted By A Diffusion With Absorption Model Involving A Moving Free Boundary

B. H. Arve

Athanasios I. Liapis
Missouri University of Science and Technology, ail@mst.edu

Recommended Citation

B. H. Arve and A. I. Liapis, "Oxygen Tension Profiles In Tumors Predicted By A Diffusion With Absorption Model Involving A Moving Free Boundary," *Mathematical and Computer Modelling*, vol. 10, no. 3, pp. 159 - 174, Elsevier, Jan 1988.
The definitive version is available at https://doi.org/10.1016/0895-7177(88)90020-9

Mathl Comput. Modelling, Vol. 10, No. 3, pp. 159–174, 1988
Printed in Great Britain

0895-7177/88 $3.00 + 0.00
Pergamon Press plc

OXYGEN TENSION PROFILES IN TUMORS PREDICTED BY A DIFFUSION WITH ABSORPTION MODEL INVOLVING A MOVING FREE BOUNDARY

B. H. ARVE† and A. I. LIAPIS‡
Department of Chemical Engineering and Biochemical Processing Institute, University of Missouri-Rolla, Rolla, MO 65401-0249, U.S.A.

(*Received May 1986*)

Communicated by X. J. R. Avula

Abstract—The dynamic behavior of the oxygen tension distribution in tumors during radiotherapy is studied by the development and solution of a diffusion with absorption model involving a moving free boundary. The oxygen uptake rates within the tumor are considered to be functions of the oxygen concentration and results are presented for zeroth-, half-, first- and second-order rates of absorption, as well as when the rate of oxygen absorption is described by the Michaelis–Menten expression.

The results presented in this work may be used together with the data from the oxygen radiosensitivity curve of a tumor, in order to determine the proper radiation dosage that should be applied to the tumor during radiotherapy, so as to compensate for the lost killing effectiveness resulting from oxygen consumption by the tumor. The model used in this study may also be employed in examining the role of oxygen and hypoxia in chemotherapy, when cycle-specific chemotherapeutic agents are used.

The numerical procedure developed for the solution of the equations of the model may become applicable to problems encountered in such diverse areas as statistical decision theory, heat transfer with changes of phase, thermal explosions, optimal control and fluid flow in porous media.

NOMENCLATURE

$C(x,t)$ = Oxygen concentration in the tumor
C_0 = Oxygen surface concentration during the loading phase
D = Effective diffusion coefficient of oxygen in tumor
D_i = Effective diffusion coefficient of oxygen in region i of a tumor with multiple regions
$f(C)$ = Rate of consumption of oxygen per unit volume of absorbing tissue
$g(\theta)$ = Dimensionless rate of consumption of oxygen
k = Michaelis constant
K = Dimensionless constant defined in equation (26)
L_i = Length of region i of a tumor with multiple regions
n = Total number of regions in a tumor with multiple regions
N = Number of internal collocation points
N_{O_2} = Flux of oxygen at the surface of the tumor during the loading phase (kg/m^{2}s)
$P_N(\xi)$ = Orthogonal polynomial
$q(x)$ = Oxygen tension distribution in the tumor at steady state (kg/m^3)
t = Time
t_f = Total time required for the moving free boundary to recede to the surface of the tumor
V = Maximum oxygen absorption rate
$X, X(0)$ = Innermost oxygen penetration in the steady-state phase
x = Spatial position
$X(t)$ = Position of the moving free boundary
y = Dimensionless spatial position
$y_0(\tau)$ = Dimensionless position of the moving free boundary

Greek symbols
α = Constant in equation (3)
β = Constant in equation (3)
γ_i = Solubility coefficient of oxygen in region i
δ = Dimensionless oxygen concentration at the moving free boundary
$\rho = (\alpha/D)^{1/2}$; constant defined in equation (13)
θ = Dimensionless oxygen concentration
λ_1 = Dimensionless constant defined in equation (25)
λ_2 = Dimensionless constant defined in equation (26)
ξ = Dimensionless space variable defined in equation (27)
τ = Dimensionless time
τ_f = Total dimensionless time required for the moving free boundary to recede to the surface of the tumor

Superscripts
s = Form factor; 0, 1 and 2 for slab, cylinder and sphere, respectively

Subscripts
i = Index for regions in a tumor with multiple regions

† Present address: Pharmacia AB, Biotechnology, Research Department, 75182 Uppsala, Sweden.
‡ To whom all correspondence should be addressed.

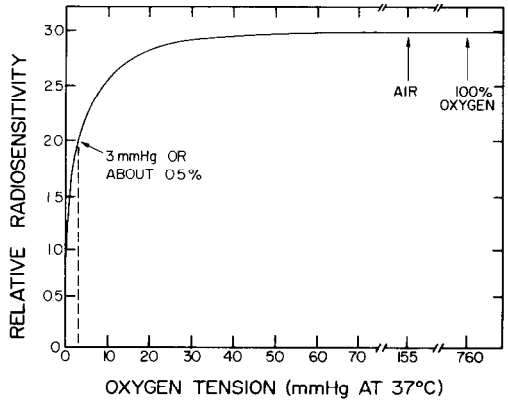

Fig. 1. Relative radiosensitivity vs oxygen tension. (From Hall [3, p. 85], courtesy of Harper & Row.)

INTRODUCTION

In the treatment of cancer by radiotherapy the aim is to apply a radiation dosage large enough to kill the cancerous cells without damaging surrounding healthy cells, and still remain within the tissue tolerance level of radiation. The susceptibility of cancerous cells to radiation has been shown to increase with increasing oxygen concentrations within the tumor [1–4] and this is illustrated in Fig. 1, taken from Hall [3]. It is observed (Fig. 1) that a steep variation occurs at low oxygen tensions with an optimum radiosensitivity at an oxygen tension of approx. 30 mmHg. If hypoxic cells represent a significant fraction of the cell population in a tumor, then a large number of cells would survive administered radiation. These cells, during tumor regression, will come closer to the underlying stroma, reoxygenate and then enter the cell cycle causing tumor regrowth. In general [3], about two or three times more radiation is needed to kill hypoxic cells than well-oxygenated cells.

For more than 50 years the role of oxygen in tumor biology has been the subject of investigation of many researchers in the biological sciences. The experimental results of several investigators [5, 6] suggest that cell systems with a high rate of cell division generally suffer the most radiation damage. Therefore, hypoxic cells should be less sensitive to radiation than well-oxygenated cells which enter the cell cycle more frequently. Other studies [3, 7–9] indicate that the organic free radical $R^{\cdot}$ which results from incident radiation or from interaction with a hydroxy free radical, interacts with oxygen in the following apparent reaction:

$$R^{\cdot} + O_2 \rightarrow RO_2^{\cdot}.$$

The radiation damage is fixed because the organic peroxy radical cannot easily be repaired. Thus, the role of oxygen to tumors appears to be twofold and numerous investigations show that hypoxia confers resistance on cells that would otherwise be sensitive to radiation therapy [4, 10, 11].

Hypoxic cells have also been found to be significantly more resistant than well-oxygenated cells to cycle-specific chemotherapeutic agents like bleomycin, cyclophosphamide, adriamycin and actinomycin [12–14]. This finding may be explained by the fact that certain chemotherapeutic agents require a singlet oxygen or superoxide radical as an intermediate to act on cell structures as well as by the observation that cells with a low oxygen tension progress slowly through the cell cycle [15] and sometimes are arrested altogether. Therefore, the role of oxygen is also of paramount importance in chemotherapy when cycle-specific chemotherapeutic agents are used.

While most normal cells are well-oxygenated, many tumors grow in solid masses which are not penetrated by blood capillaries and oxygen will have to reach the inner parts of the tumor by diffusion. Depending on the size and type of the cancer, there may be parts within the tumor where the oxygen concentration is very low or approximately zero [16]. Gatenby *et al.* [17] made *in vivo* measurements of oxygen tension profiles within human tumors and their results indicate that in large tumors which have significantly outgrown their blood supply, the size of the well-oxygenated rim is quite small when compared to the size of the thick tumor mass characterized by hypoxic

cells. The technique developed by Gatenby *et al.* [17] uses a CT-guided polarographic probe and the location of each measurement is documented by demonstrating the position of the tip of the probe with a CT scan. Measurements of oxygen concentration in tissues using polarographic methods have also been reported by Carter and Silver [18], Evans and Naylor [19], Constable and Evans [20] and Mueller-Klieser *et al.* [4].

The use of oxygen in human cancer radiotherapy was first reported by Hultborn and Forssberg [21]. One-half of the tumor was irradiated with the patients breathing air at atmospheric pressure and the other half while they were breathing pure oxygen (also at atmospheric pressure). It was shown that the radiation effect was markedly enhanced in the half of the tumor treated while the patients were breathing pure oxygen. Similar results have been shown by Churchill-Davidson *et al.* [22] and Van Den Brenk *et al.* [23]. The studies of these investigators led to the use of hyperbaric oxygen in combination with radiation in tumor therapy. Hyperbaric oxygen proved to be an efficient tool for improving the oxygen supply to tumor tissue and for eradicating hypoxia in solid tumors [24–27].

Even though intensive research [4] has been directed towards radiosensitizing drugs that could replace oxygen application and hyperbaric oxygen, respectively, in improving the radiosensitivity of solid tumors, hyperbaric oxygen is still being considered a quantitatively effective and relevant radiosensitizer. In a comparative study, Suit *et al.* [28] showed that there was no benefit in using misonidazole at clinical doses compared to hyperbaric oxygen at 3 bar. Despite some controversies in this regard [29], and taking into account side-effects of radiosensitizers, such as neurotoxicity, it is concluded that the development of radiosensitizing drugs has not yet reached a level of general clinical applicability, comparable to that of hyperbaric oxygen.

While a significant number of experimental studies have been reported where the oxygen distribution within tissue has been measured and several techniques have been developed for the detection and measurement of hypoxic cells in solid tumors [30], very few attempts have been made in predicting theoretically the oxygen tension profiles within solid tumors that result from increasing the oxygen level through the supply of pure oxygen under atmospheric or hyperbaric conditions as well as during radiotherapy [31–33]. The predictions of theoretical models would be of interest in clinical radiotherapy and could be used to gain insight into the roles of oxygen and hypoxia in the response of tumors to radiotherapy, and even to chemotherapy when cycle-specific chemotherapeutic drugs are used.

PROBLEM STATEMENT

The method of interest for introducing oxygen within solid tumors involves exposing a surface of the tumor to a high oxygen concentration [3, 35], often under high pressure, and allowing the tumor to absorb oxygen until a steady-state condition is reached where no further penetration of oxygen into the tissue occurs. This steady state is characterized by a particular oxygen profile within the tumor, resulting from internal consumption of the absorbed oxygen by cancerous cells and the diffusional resistance to oxygen transport within the tumor. Therefore, the surface may be considered to have an oxygen tension proportional to that of the oxygen source [34] and a point exists within the tissue at which the oxygen concentration has dropped to a value close to zero, marking the point of innermost penetration. Once this steady state occurs, the outer surface is sealed off and radiation treatment may begin. During the period of radiotherapy, the oxygen within the tumor continues to be consumed as well as to diffuse because of the existing, although decreasing, oxygen concentration gradient. As a consequence of the removal of oxygen, the initial steady-state profile changes and the point of innermost penetration where the oxygen tension is about zero will gradually move towards the sealed surface until no oxygen remains.

The objective of this work is to obtain information about the oxygen tension distribution within the solid tumor and how it changes with time during radiotherapy, by modeling and solving the combined diffusion and absorption processes. The predictions of the model would provide knowledge of how deep into the tumor the oxygen penetrates, how this depth depends on the oxygen concentration of the source and how the oxygen tension profile varies with time during the application of radiation.

With this information one may determine *a priori* the safe oxygen tension of the source so as to

achieve an initial oxygen penetration depth that is beyond the thickness of the solid tumor, and the time at which the oxygen concentration within the tumor has decreased to a critical low value below which the oxygen effect is negligible and thus, the treatment should be discontinued. The model predictions would also show how the oxygen concentration changes with time at each point within the tumor and therefore, by knowing how the radiosensitivity changes with oxygen tension, a time-varying radiation dosage may be established so as to maintain the desired effectiveness of the radiation treatment.

MATHEMATICAL FORMULATION

It has been shown that for oxygen the role of diffusion is significantly more important than that of convection in most tumors [4, 33, 36–42]. Therefore, the complex transport mechanisms of oxygen in absorbing tumors may be simplified by assuming that the transport of oxygen is governed by diffusion. The transport mechanism is taken to be one-dimensional and it is assumed that local equilibrium exists between the tissue and oxygen at each point, since the process of absorption is rarely rate limiting [34, 35, 43]. Also, the diffusion with absorption process is taken to be isothermal.

The continuity equation derived from a differential oxygen mass balance in the absorbing tumor, is given by the partial differential equation

$$\frac{\partial C}{\partial t} = \frac{1}{x^s}\frac{\partial}{\partial x}\left(x^s D \frac{\partial C}{\partial x}\right) - f(C), \tag{1}$$

where $C(x, t)$ denotes the concentration of oxygen in the tissue, D is the effective diffusion coefficient of oxygen and $f(C)$ represents the rate of consumption (absorption) of oxygen via cell respiration per unit volume of absorbing tissue. The oxygen consumption is assumed to be independent of glycolysis, and equation (1) is applicable for a slab, cylinder or sphere by setting $s = 0$, 1 or 2.

The *in vivo* measurements of steady-state oxygen tension profiles within tumors reported by Gatenby *et al.* [17] suggest that in certain tumors a diffuse trend may exist in cell morphology from the rim of the tumor (well-oxygenated cells) to a region where no cell respiration occurs (necrotic region). King *et al.* [44] have suggested that for these tumors simple multiregion type models may have practical utility but the solutions of their model have been obtained under steady-state conditions only. In this case, equation (1) could be used for each region of the tumor and should be written as follows:

$$\frac{\partial C_i}{\partial t} = \frac{1}{x^s}\frac{\partial}{\partial x}\left(x^s D_i \frac{\partial C_i}{\partial x}\right) - f_i(C_i), \qquad i = 1, 2, 3, \ldots, n, \tag{2}$$

where i denotes the various regions of the tumor (i.e. regions of well-oxygenated cells, hypoxic cells and necrotic cells) and n represents the total number of regions within a particular solid tumor. The effective diffusivity of the well-oxygenated region, where a higher degree of vascularity occurs, should be larger than the diffusivities of the other regions and may be thought of as being like an advection coefficient which lumps oxygen transport via blood flow and diffusion. In the hypoxic region there is sparse vascularity and the contribution of oxygen transport by blood flow is insignificant, while in the necrotic region where no cell respiration occurs the rate of consumption of oxygen is zero.

The present work concerns itself with slab geometry, as shown in Fig. 2. The solid tumor is considered to be dominated by the region of hypoxic cells, and the effective diffusivity of the oxygen in the solid tumor is taken to be constant. Liapis *et al.* [45] studied the case where the rate of oxygen consumption per unit volume of the absorbing tissue is constant [$f(C) = \text{const}$]. However, experimental data [17, 34, 44] indicate that the rate of oxygen consumption by cancerous cells can be a function of the oxygen tension. The present work takes this into account by considering two different expressions for the rate of oxygen absorption. The first is given by the Freundlich equation

$$f(C) = \alpha C^{\beta}, \tag{3}$$

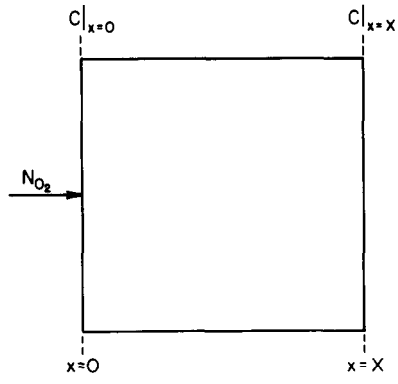

Fig. 2. One-dimensional slab representing the tumor, with X indicating the position of the moving free boundary at the end of the oxygen loading phase.

where α and β are constants determined from experimental data. Since β usually lies in the range of 0–2 [44,46], the cases presented in this work are for $\beta = 0.0$, 0.5, 1.0 and 2.0. In certain tissues the rate of oxygen absorption is described by the Michaelis–Menten [34,44,46] expression, given by

$$f(C) = \frac{VC}{k + C}, \tag{4}$$

where V and k are the maximum oxygen absorption rate and Michaelis constant, respectively. For $k = 1$, equation (4) becomes the well-known Langmuir expression. For oxygen tensions with values $\ll k$, the behavior is similar to that for equation (3) with $\beta = 1.0$, whereas for concentrations $\gg k$ it resembles the case where $f(C) = \text{const}$, i.e. where $\beta = 0.0$.

The combined oxygen diffusion and absorption mechanisms described above, are considered to be active during the loading stage of oxygen into the solid tumor (steady-state phase of the problem) as well as during radiation treatment (unsteady-state phase of the problem).

The problem involving a solid tumor with multiple regions [equation (2)] is beyond the scope of the present work, but its solution may be obtained by using the procedures presented in the following sections for a single region, together with the conditions of continuity of oxygen fluxes at the interface between regions given by

$$D_i \frac{\partial C_i}{\partial x} = D_{i+1} \frac{\partial C_{i+1}}{\partial x} \qquad \text{at } x_0 = L_i, i = 1, 2, \ldots, n-1, \tag{5}$$

and appropriate solubility-type conditions at the region interfaces like,

$$C_{i+1} = \gamma_{i+1,i} C_i \quad \text{at } x_i = L_i, \qquad i = 1, 2, \ldots, n-1. \tag{6}$$

If $\gamma_{i+1,i} = 1 \quad \forall i$, this implies the continuity of the oxygen tension at the interface between regions.

Steady-state phase

During the initial phase when oxygen is being loaded into the tumor, the oxygen tension at the surface has a constant value C_0,

$$C = C_0 \qquad \text{at } x = 0. \tag{7}$$

A steady state is reached when the concentration gradient becomes zero at a point X in the slab where the oxygen tension is also zero. At steady state the concentration at every point in the tumor becomes independent of time, i.e. the accumulation term is zero everywhere since at this state the rates of absorption and diffusion are equal to the rate of oxygen supply from the source. The point

X marks the innermost penetration of oxygen and no oxygen can diffuse beyond this point. Therefore, the following conditions exist:

$$\frac{\partial C}{\partial x} = 0 \qquad \text{at } x = X \tag{8}$$

$$C = 0 \qquad \text{at } x = X. \tag{9}$$

The steady-state solution is obtained by solving

$$D\frac{\partial^2 C}{\partial x^2} - f(C) = 0, \tag{10}$$

subject to the boundary conditions given by equations (7) and (8); equation (9) is employed in the calculation of the innermost penetration X. For the case where $f(C) = \alpha C^{\beta}$ and $\beta = 0.0$ [31,45], the solution of equation (10) gives

$$C = \frac{\alpha}{2D}(x - X)^2, \tag{11}$$

where

$$X = \left(\frac{2DC_0}{\alpha}\right)^{1/2}. \tag{12}$$

When $\beta = 1.0$, the solution of equations (7), (8) and (10) leads to the following expression:

$$\frac{C}{C_0} = \frac{\cosh[\rho(x - X)]}{\cosh(\rho X)}, \tag{13}$$

where $\rho^2 = \alpha/D$. The boundary condition in equation (9) is satisfied as $X \to \infty$ in equation (13). This may also be the case for other forms of $f(C)$.

An approximate solution to a problem with this property ($C \to 0$ as $X \to \infty$) can be obtained with a specified degree of accuracy, by incorporating the idea of innermost penetration where the oxygen tension is as small as desired but nonzero [47, p. 67]. This implies that a deepest point of penetration may be found at a finite length X where C is very small and close to zero, and the oxygen tension distribution beyond this point may be neglected. This approximation also makes it possible to trace a minimum (critical) oxygen concentration within the tumor below which the oxygen effect is negligible. Therefore, X can be estimated from equation (13) by letting $C/C_0 = \delta$, where δ is taken to be a small number close to zero. When X has been estimated, equation (13) provides the steady-state oxygen tension distribution with $C = C_0$ at $x = 0$, and $C = \delta C_0$ at $x = X$.

For cases where the rate of oxygen absorption, $f(C)$, is a nonlinear function of the oxygen tension, the steady-state profile is obtained by solving equation (10) numerically so as to give a concentration profile which is cut off at a penetration depth X where the oxygen tension is δC_0. The range of values of C_0 may vary between 1.25×10^{-3} and 4.97×10^{-3} g/cm^3 [3,4], and Arve [46] in his calculations varied the value of δ between 10^{-3} and 10^{-4}.

Unsteady-state phase

Once the surface ($x = 0$) is sealed off and radiation is applied, no more oxygen is allowed to enter the solid tumor but oxygen already present in the tissue, continues to be consumed and diffuse. Therefore, the point of innermost penetration, X, moves towards the surface of the slab.

This part of the process can be represented by the following equations:

$$\frac{\partial C}{\partial t} = D\frac{\partial^2 C}{\partial x^2} - f(C), \qquad 0 \leqslant x \leqslant X(t), t > 0; \tag{14}$$

$$\frac{\partial C}{\partial x} = 0 \qquad \text{at } x = 0,\ t > 0; \tag{15}$$

$$\frac{\partial C}{\partial x} = 0 \qquad \text{at } x = X(t),\ t > 0; \tag{16}$$

$$C = 0 \qquad \text{at } x = X(t),\ t > 0; \tag{17}$$

$$C = q(x) \qquad \text{at } t = 0,\ 0 \leqslant x \leqslant X(0); \tag{18}$$

where the function $q(x)$ is the oxygen tension distribution obtained from the steady-state phase, and is given by equation (12) when $\beta = 0.0$ and by equation (13) when $\beta = 1.0$.

It should be noted that the innermost penetration X of the steady-state phase corresponds to $X(0)$ of the unsteady-state phase, and the boundary condition given by equation (17) takes the form

$$C = \delta C_0 \qquad \text{at } x = X(t), t > 0, \tag{17'}$$

for the case where $\beta = 1.0$ or when $f(C)$ leads to a solution of the steady-state phase, such that $C \to 0$ only as $X \to \infty$.

The above equations can be put in dimensionless form by defining the following variables:

$$y = \frac{x}{X(0)}, \qquad \tau = \frac{Dt}{(X(0))^2}, \qquad \theta = \frac{C}{C_0}, \qquad y_0(\tau) = \frac{X(t)}{X(0)}, \tag{19}$$

where $y_0(\tau)$ represents how the position of the innermost penetration changes with time, τ. Equations (14)–(18) then become:

$$\frac{\partial \theta}{\partial \tau} = \frac{\partial^2 \theta}{\partial y^2} - g(\theta), \qquad 0 \leqslant y \leqslant y_0(\tau), \tau > 0; \tag{20}$$

$$\frac{\partial \theta}{\partial y} = 0 \qquad \text{at } y = 0, \tau > 0; \tag{21}$$

$$\frac{\partial \theta}{\partial y} = 0 \qquad \text{at } y = y_0(\tau), \tau > 0; \tag{22}$$

$$\theta = 0 \qquad \text{at } y = y_0(\tau),\ \tau > 0; \tag{23}$$

$$\theta = q(y) \qquad \text{at } \tau = 0,\ 0 \leqslant y \leqslant y_0(0); \tag{24}$$

where $y_0(0) = 1.0$, and the function $g(\theta)$ has the forms

$$g(\theta) = \lambda_1 \theta^{\beta}, \qquad \lambda_1 = \frac{(X(0))^2 \alpha (C_0)^{\beta - 1}}{D}, \tag{25}$$

and

$$g(\theta) = \lambda_2 \left(\frac{\theta}{K + \theta}\right), \qquad \lambda_2 = \frac{(X(0))^2 V}{DC_0}, \qquad K = \frac{k}{C_0}. \tag{26}$$

The form given in equation (25) is used when $f(C)$ is represented by the Freundlich expression, while equation (26) is employed in the case where $f(C)$ follows the Michaelis–Menten equation. When the absorption rate $f(C)$ is such that $C \to 0$ when $X(0) \to \infty$ in the steady-state phase, then the boundary condition given by equation (23) should become

$$\theta = \delta \qquad \text{at } y = y_0(\tau), \tau > 0. \tag{23'}$$

The function $q(y)$ is given by

$$q(y) = \frac{\lambda_1}{2}(1 - y)^2 \tag{11'}$$

when $\beta = 0.0$, and by

$$q(y) = \frac{\cosh[\rho X(y - 1)]}{\cosh(\rho X)} \tag{13'}$$

for the case where $\beta = 1.0$. The numerical solution of the expressions given by

$$\theta = 1 \qquad \text{at } y = 0, \tag{7'}$$

$$\frac{\partial \theta}{\partial y} = 0 \qquad \text{at } y = 1, \tag{8'}$$

$$\theta = 0 \qquad \text{at } y = 1 \tag{9'}$$

and

$$\frac{\partial^2 \theta}{\partial y^2} - g(\theta) = 0, \qquad 0 \leqslant y \leqslant 1, \tag{10'}$$

would provide the function $q(y)$ when analytical solutions of the steady-state phase are not available. It is important to note that when $g(\theta)$ is such that $\theta = 0$ only for $X(0) = \infty$, the boundary condition given by equation (9') takes the form,

$$\theta = \delta \qquad \text{at } y = 1. \tag{9''}$$

The system of equations (20)–(24) represents a moving boundary problem since the point of innermost penetration, $X(t)$, moves towards the surface as time progresses. Because there is no oxygen diffusing across the moving boundary at any time and since the oxygen tension is zero at the boundary, there is no relationship which contains the velocity of the moving boundary explicitly.

Moving boundary problems are often tedious and difficult to solve [47–51]. Often, Crank–Nicholson or other finite-difference numerical schemes are used [31, 52]. These numerical methods usually require large computation times and are often applicable only when the velocity of the moving boundary is small. In general, the moving boundary will not coincide with a grid in successive time steps, $\Delta\tau$, if $\Delta\tau$ is taken to be constant and predetermined. Because of these limitations, the solution and parameter estimation of models which involve moving boundaries have been, in most cases, intractable.

Numerical solution procedure

The numerical method of orthogonal collocation [53, 54] is used to solve the differential equations of the steady-state and unsteady-state phases. The method of orthogonal collocation is easier to apply to problems with model equations of fixed extent than it is to problems with changing domains. Equation (20) can have a domain of fixed extent if the position of the moving boundary,

$y_0(\tau)$, is fixed, by defining a new space variable as follows [45, 46]:

$$\xi = \frac{y}{y_0(\tau)}. \tag{27}$$

The transformed model equations of the unsteady-state phase are:

$$\frac{\partial\theta}{\partial\tau} = \frac{1}{[y_0(\tau)]^2}\frac{\partial^2\theta}{\partial\xi^2} + \frac{\xi}{y_0(\tau)}\left[\frac{dy_0(\tau)}{d\tau}\right]\frac{\partial\theta}{\partial\xi} - g(\theta), \qquad 0 \leqslant \xi \leqslant 1, \tau > 0; \tag{28}$$

$$\frac{\partial\theta}{\partial\xi} = 0 \qquad \text{at } \xi = 0, \tau > 0; \tag{29}$$

$$\frac{\partial\theta}{\partial\xi} = 0 \qquad \text{at } \xi = 1, \tau > 0; \tag{30}$$

$$\theta = 0 \qquad \text{at } \xi = 1, \tau > 0; \tag{31}$$

$$\theta = q(\xi) \qquad \text{at } \tau = 0, 0 \leqslant \xi \leqslant 1. \tag{32}$$

The function $q(\xi)$ is obtained from the solution of the following transformed equations of the steady-state phase:

$$\frac{\partial^2\theta}{\partial\xi^2} - g(\theta) = 0, \qquad 0 \leqslant \xi \leqslant 1; \tag{33}$$

$$\theta = 1 \qquad \text{at } \xi = 0; \tag{34}$$

$$\frac{\partial\theta}{\partial\xi} = 0 \qquad \text{at } \xi = 1; \tag{35}$$

$$\theta = 0 \qquad \text{at } \xi = 1. \tag{36}$$

If the function $g(\theta)$ is such that $\theta = 0$ when $X(0) = \infty$, then the boundary condition in equations (31) and (36) should take the form

$$\theta = \delta \qquad \text{at } \xi = 1. \tag{37}$$

The method of orthogonal collocation was applied on the space variable and the approximation order N of the Jacobi orthogonal polynomials $P_N(\xi)$ ranged from 18 to 58 for the different cases studied. The position of the moving boundary is determined by trial and error (since there is no explicit expression for its velocity), so as to satisfy the boundary condition given by equations (31) and (36) or (37). The details of the numerical procedures used to solve equations (28)–(37) and their computer program are presented in Arve's [46] thesis.

RESULTS AND DISCUSSION

In Fig. 3 the innermost penetration, $X(0)$, during the steady-state phase as well as the total time, t_f, that it takes for the moving boundary to proceed from $X(0)$ to the surface of the tumor during the unsteady-state phase, are plotted against the absorption parameter β. The results are shown for two different oxygen loading tensions, and the value of the effective diffusivity, D, is within the range of values estimated for various tumors [1, 44]. The values of the oxygen loading tension, C_0, used in the model simulations, are characteristic of those used in clinical radiotherapy [4, 55], while

the value of α is taken to be 1 in the numerical experiments reported in this work. The values of the kinetic parameter β are varied between 0 and 2, since the experimental data of Gatenby *et al.* [17] and King *et al.* [44] suggest that the order, β, of oxygen absorption in tumors is within the above-mentioned interval.

The oxygen concentration throughout the slab is always $< C_0$ because of the continuous consumption of oxygen in the tumor. Therefore, in the range of $C_0 < 1$, the rate of absorption in a tumor with a small β will be greater than in a tumor with a large β at a given oxygen tension. Thus, the mechanism of diffusion in a tumor with a large value of β will allow the oxygen to penetrate deeper into the tumor, before the oxygen concentration reaches the prescribed value δC_0. As a result, when $C_0 < 1$, the penetration depth, $X(0)$, increases with increasing absorption order and this is clearly shown in Fig. 3. When $\beta = 1$, the value of $X(0)$ is the same for both values of C_0, because for a selected value of δ equation (13) will provide the same innermost penetration for all values of C_0.

The effect of β on the total time, t_f, that it takes for the free boundary to move to the surface of the tumor during the unsteady-state phase is similar to the effect of β on $X(0)$, as shown in Fig. 3. From equation (19) it is observed that the time variable, t, is proportional to the square of $X(0)$ and varies linearly with the dimensionless time, τ. The dimensionless total time, τ_f, was found to be of the same magnitude for all values of β shown in Fig. 3 [46], and this together with equation (19) can explain the similarities in the behavior of t_f and $X(0)$ as β and C_0 vary. The total time, t_f, varies substantially for different values of β since the rate of absorption decreases as β increases in this range of C_0. Therefore, it takes a longer time to consume the oxygen that is present in the tumor for a larger β, and also for values of $C_0 < 1$ the total amount of oxygen at the beginning of the unsteady-state phase is larger as the value of β increases.

The position of the moving boundary as a function of the dimensionless time, τ, is shown in Fig. 4. It is observed that the qualitative dynamic behavior of the free boundary is the same for all values of β, and Arve [46] has shown that the same dynamic behavior as that shown in Fig. 4 is obtained when the absorption rate is given by the Michaelis–Menten expression. The velocity of the free boundary, given by the slope of the curve, is at first very small and as time proceeds it approaches infinity. This behavior occurs because oxygen is continuously consumed with the tendency to move the boundary towards the surface of the slab, but the movement is initially counteracted by the diffusion process. As the oxygen tension decreases the absorption process is gradually overtaking the effect of diffusion, and when all the oxygen has been consumed the free boundary has moved to the surface. A close study of the data shown in Fig. 4 indicates that in all cases the free boundary has moved at most 20% from its initial position, when 70% of the total time of the unsteady-state phase has elapsed. The velocity of the moving boundary, $X(t)$ can be

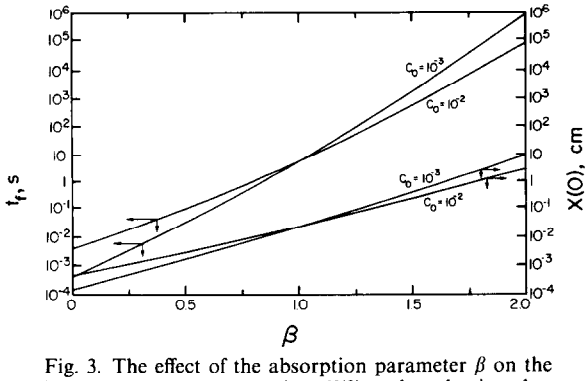

Fig. 3. The effect of the absorption parameter β on the innermost oxygen penetration, $X(0)$, and on the time that is required for the free boundary to move to the tumor surface during the application of radiation. $\alpha = 1$ $(g/cm^3)^{1-\beta}/s$, $D = 10^{-5}\,cm^2/s$, $\delta = 10^{-3}$; the units of C_0 are g/cm^3.

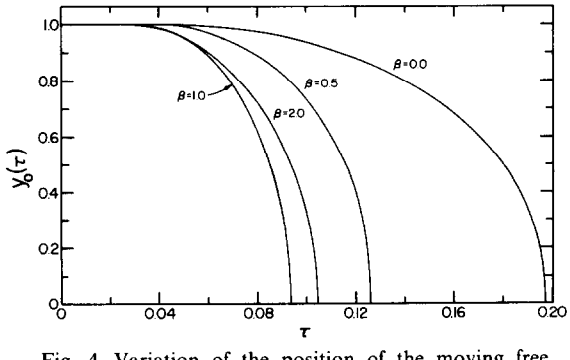

Fig. 4. Variation of the position of the moving free boundary, $y_0(\tau)$, with dimensionless time, τ (Freundlich equation, $\delta = 10^{-3}$).

evaluated by the following expression:

$$\frac{dX(t)}{dt} = \frac{D}{X(0)} \frac{dy_0(\tau)}{d\tau}. \tag{38}$$

Thus, for a given time t, one calculates τ from equation (19) and the slope $dy_0(\tau)/d\tau$ at τ is estimated from a curve similar to those shown in Fig. 4; then the velocity of the free boundary at t is calculated from equation (38). It is important to note that the data shown in Fig. 4 represent the behavior of nondimensional variables, and the real-time interpretation of these results should consider the appropriate use of these data with equation (19).

The numerical experiments of Arve [46] show that the value of C_0 does not only affect the penetration depth $X(0)$ and the total time, t_f, as shown in Fig. 3, but also the time at which the free boundary starts to move appreciably during the unsteady-state phase. Therefore, it may be possible for a given oxygen absorption rate function $f(C)$ and effective diffusivity D, to select a safe oxygen tension C_0 so that the minimum concentration required for an oxygen effect during radiation treatment is located beyond the innermost depth of the tumor, and also C_0 is such that the free boundary does not start to move significantly until the radiation treatment is completed. This would imply that a constant radiation dosage may be used during radiotherapy. If the properties of the tissue are such that oxygen cannot penetrate through the length of the tumor when medically safe values of C_0 are used and the times for establishing the oxygen tension profiles of the steady-state phase are within an acceptable time interval for oxygen loading, then a time-varying radiation dosage should be used to compensate for the loss of the effectiveness of radiation due to the depletion of oxygen in the tumor.

The oxygen tension profiles in the tumor are presented for different dimensionless times, τ, in Figs 5–10; the Michaelis–Menten parameter K in Figs 9 and 10 is given by $K = k/C_0$, and the value of V in equation (4) is taken to be 1 g/cm^{3}s. From Fig. 8 it is clearly observed that for $\beta = 2.0$ the oxygen concentration of the steady-state phase ($\tau = 0.0$) is very low for a large part of the slab, and changes significantly only in the neighborhood of the surface during the unsteady-state phase. This occurs because of the strong dependence of the rate of absorption on oxygen tension, which results in large differences in magnitude of the absorption rate within the slab. The difference is 10^6-fold between the surface and the point of innermost penetration at steady state for $\beta = 2.0$. However, the rate of absorption is a weak function of oxygen concentration when β is small, and therefore the differences in the absorption rates within the tumor are small. As a result, the oxygen tension is fairly large even close to the innermost boundary (Figs 5 and 6).

As time progresses the oxygen tension gradient that defines the diffusional flux decreases because of the continuous consumption of oxygen. This will effect a change in the relative diffusion and absorption rates within the tumor but differently for different values of β. A comparison of the results when $\tau = 0.001$, shows that only small amounts of oxygen have been consumed for the cases where $\beta = 0.0$ and 0.5 (Figs 5 and 6); for the larger values of β, the amount of oxygen

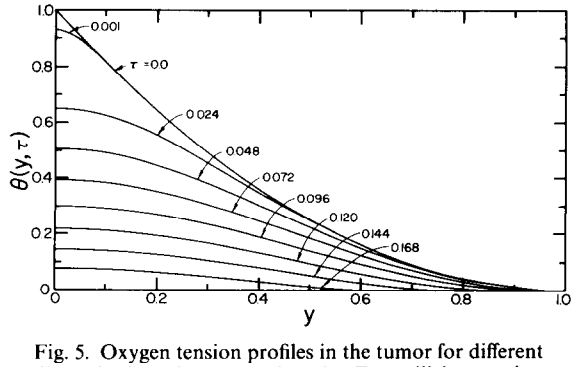

Fig. 5. Oxygen tension profiles in the tumor for different dimensionless times, τ, using the Freundlich equation with $\beta = 0.0$.

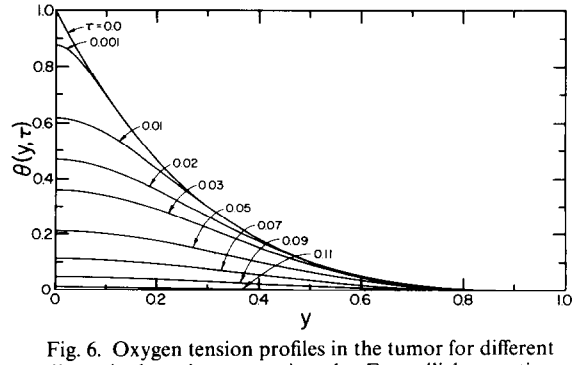

Fig. 6. Oxygen tension profiles in the tumor for different dimensionless times, τ, using the Freundlich equation with $\beta = 0.5$ ($\delta = 10^{-3}$).

consumed is greater and for $\beta = 2.0$ (Fig. 8) most of the oxygen has been absorbed.

It is also interesting to note how much the dimensionless surface concentration has decreased before the free boundary starts to move significantly. For $\beta = 0.0$ and 0.5 the free boundary has moved 10% from its initial position, when the surface concentration has dropped to 24 and 8.2% of the initial value of C_0, respectively. The corresponding values for $\beta = 1.0$ and 2.0 are 0.96 and 0.17%. This occurs because for higher values of β the real time that it takes for the free boundary to move 10% from its initial position is significantly larger than the time required for lower values of β, since the innermost penetration $X(0)$ is much higher for larger values of β (Fig. 3). Therefore, because of these larger-dimensional times the concentration of oxygen at every point in a tumor with a high β value, is much lower than that encountered when the value of β is low.

A comparison of the oxygen tension profiles shown in Figs 9 and 10 with those in Figs 5–7, indicates that for a small K the results obtained with the Michaelis–Menten absorption rate fall in between the calculated data using the Freundlich expression with $\beta = 0.0$ and 0.5. For the higher value of K (Fig. 10), the results in nondimensional form are closer to the case where $\beta = 1.0$. However, the results in dimensional form for $K = 5.0$ vary substantially from the case where $\beta = 1.0$ [46].

The variation of the dimensionless oxygen tension at the surface of the tumor with dimensionless time, τ, is shown in Figs 11 and 12; in Fig. 12 the data for $\beta = 0.0$ and 1.0 are also included in order to compare them with the results obtained for small and large values of the Michaelis–Menten parameter K. It is observed that for large values of β the surface concentration is very low for most part of the process time, while for lower values of β the surface oxygen tension decreases less rapidly during the unsteady-state phase. The data in Fig. 12 suggest that for small values of K the dynamic behavior of the oxygen tension at the surface is qualitatively similar to that obtained with values of β close to zero, while for large values of K the dynamic behavior is similar to that

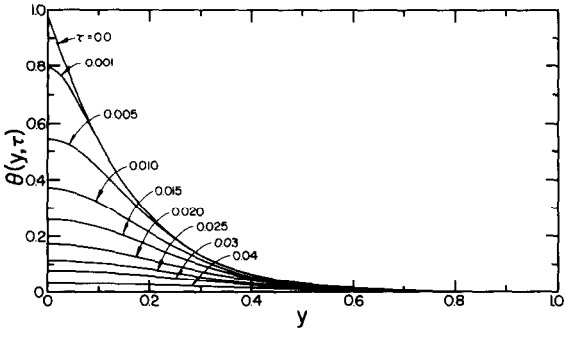

Fig. 7. Oxygen tension profiles in the tumor for different dimensionless times, τ, using the Freundlich equation with $\beta = 1.0$ ($\delta = 10^{-3}$).

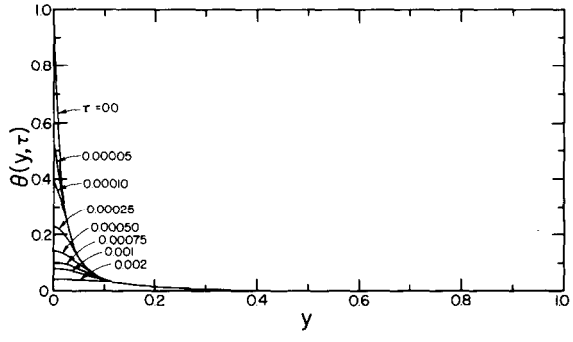

Fig. 8. Oxygen tension profiles in the tumor for different dimensionless times, τ, using the Freundlich equation with $\beta = 2.0$ ($\delta = 10^{-3}$).

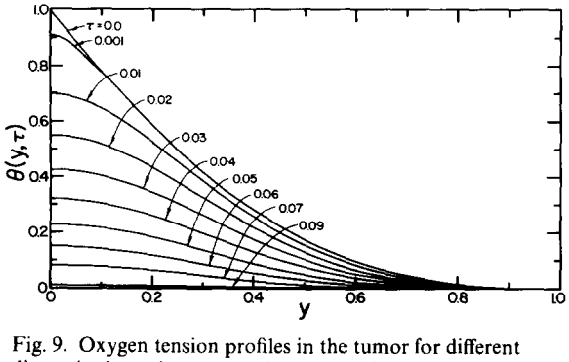

Fig. 9. Oxygen tension profiles in the tumor for different dimensionless times, τ, using the Michaelis–Menten equation with $K = 0.05$ ($\delta = 10^{-3}$).

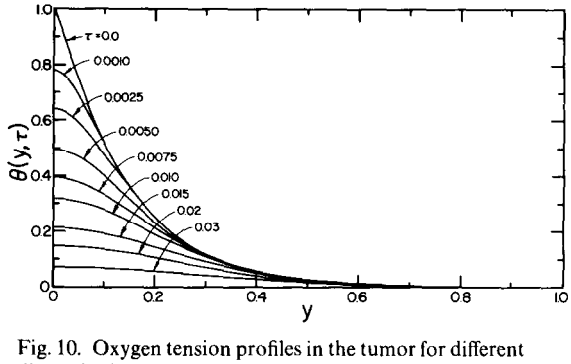

Fig. 10. Oxygen tension profiles in the tumor for different dimensionless times, τ, using the Michaelis–Menten equation with $K = 5.0$ ($\delta = 10^{-3}$).

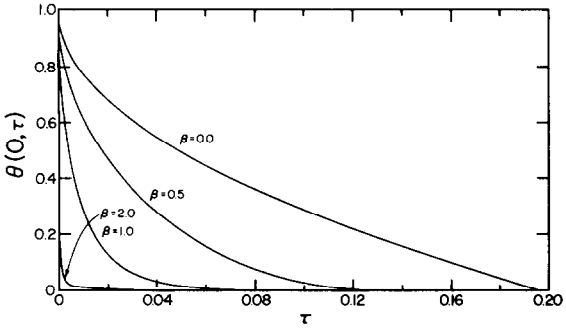

Fig. 11. Variation of the oxygen tension at the surface of the tumor with dimensionless time, τ, using the Freundlich equation ($\delta = 10^{-3}$).

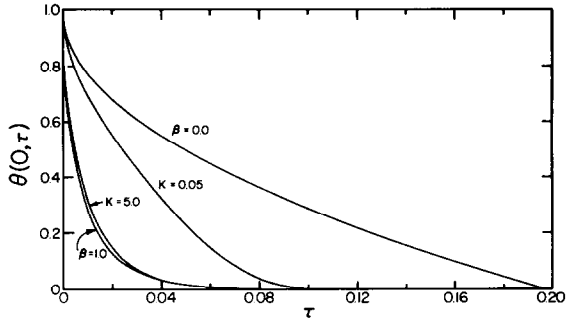

Fig. 12. Variation of the oxygen tension at the surface of the tumor with dimensionless time, τ, using the Michaelis–Menten equation ($\delta = 10^{-3}$).

obtained with $\beta = 1.0$.

With the aid of the data shown in Figs 3–12, a method to control the radiation dosage with time may be established. Since the oxygen tension decreases at every point in the tumor during radiation treatment, the radiosensitivity may change so that the effectiveness of the radiation becomes less than expected. A procedure where the applied radiation dosage is controlled by the varying oxygen concentration in the tumor could insure that the desired killing effect of the radiation is maintained throughout the time period of the treatment. In order to determine the proper radiation dosage, one must know how the radiosensitivity of the cancerous cells changes with oxygen tension (oxygen radiosensitivity curve, Fig. 1) in the tumor of interest, and how the oxygen concentration distribution varies with time in that tumor. The oxygen radiosensitivity curve may be determined experimentally [3, 56], and the information about the time variation of the oxygen tension distribution may be obtained by the model presented and solved in this work. The model parameters D, α, β, V and K may be established by the procedures reported in the literature.

When the oxygen tension profile of the steady-state phase is known, one may determine the starting radiation dosage. It may be determined so that the point within the tissue where the lethal effect of the radiation becomes insignificant (radiation penetration depth), is not beyond the point where the oxygen concentration is so low (critical oxygen tension) that the oxygen effect starts to decrease. The location of the point where the concentration becomes lower than the critical oxygen tension may be found in Figs 5–10 for the pertinent β or K, at $\tau = 0.0$. If the critical oxygen concentration is beyond the innermost boundary of the tumor at $\tau = 0.0$, then one may use a radiation dosage sufficient to effect therapy through the whole length of the tumor. However, if the oxygen tension reaches the critical concentration at a point within the tumor, then a radiation dosage should be used at $\tau = 0.0$, that effects therapy up to the point within the tumor where the oxygen concentration is greater or equal to the critical oxygen tension.

During the unsteady-state phase the data in Figs 5–10 allow one to follow how the critical concentration moves towards the surface of the tumor with time. If it is found that the time it takes for the critical oxygen tension to recede to the innermost depth of the tumor is larger than the time allowed for safe radiation treatment, then a constant radiation dosage may be used throughout the time period of radiotherapy. However, if the oxygen concentration becomes lower than the critical tension, during radiation treatment, at the radiation penetration depth, then a time-varying radiation dosage is required to maintain the desired effectiveness of radiation. In this case the radiation should be changed according to the variation of the concentration at the radiation penetration depth. When the oxygen concentration at this point has decreased to a level where the oxygen effect is negligible, then the application of radiation should be discontinued.

More results, similar to those shown in Figs 3–12 for other values of the parameters C_0, β and K as well as data showing the variation of the average oxygen concentration in the slab with time, are reported in the work of Arve [46]. The effect of the value of δ on the numerical values of the variables $X(0)$, $C(x,t)$, $X(t)$ and t_f as well as on the computational efficiency of the numerical procedure used to solve the model, is discussed in great length in the thesis of Arve [46]. Finally, it is important to note that the solution procedure presented in this work can become applicable

to problems encountered in such diverse areas as statistical decision theory [57], optimal control [58], fluid flow in porous media [59,60], heat transfer with changes of phase [61] and chemical reactions such as thermal explosions [62]. This numerical method can be extended for the solution of spatially, multidimensional diffusion with absorption or reaction problems involving a free boundary, by employing collocation on the space variables with orthogonal polynomials in multiple variables and the general transformation developed by Saitoh [49] which fixes the position of the moving boundary.

CONCLUSIONS AND REMARKS

Oxygen tension profiles in tumors are predicted by the solution of a diffusion with absorption model involving a moving free boundary. This model describes the oxygen concentration distribution and the innermost penetration of oxygen during the loading phase of oxygen in the tumor, as well as during the time period of the application of radiation. The expressions of the oxygen absorption rates are considered to be functions of the oxygen tension and results are obtained for zeroth-, half-, first- and second-order rates of oxygen uptake, as well as for absorption rates described by the Michaelis–Menten expression.

The model predictions during the loading phase of oxygen (provided from an oxygen source) into the tumor, can lead to the selection of a medically safe oxygen surface concentration which would provide a desirable oxygen tension profile and penetration depth at the end of the loading phase. This oxygen profile would determine the starting radiation dosage during the unsteady-state phase of radiation treatment.

The results describing the time variation of the oxygen tension distribution in the tumor during the application of radiation, may be used together with the oxygen radiosensitivity data of the tumor in order to determine the appropriate radiation dosage that should be administered to the tumor, so as to compensate for the lost killing effectiveness resulting from oxygen consumption by cancerous cells. The mathematical model may also be used in studies that would optimize the therapeutic effect of radiation.

Furthermore, since hypoxic cells have also been found to be significantly more resistant than well-oxygenated cells to cycle-specific chemotherapeutic agents [12–14], it becomes apparent that the model presented in this work may be used to gain insight into the role of hypoxia and the role of oxygen in the response of tumors to chemotherapy.

A discussion is also offered and certain expressions are presented that would be required in extending the applicability of the model to tumors with multiple regions [17]. Finally, the solution procedure developed for the problem presented in this work, may become applicable to problems in the areas of statistical decision theory, thermal explosions, heat transfer with changes of phase, fluid flow in porous media and optimal control.

Acknowledgments—The authors gratefully acknowledge helpful discussions with Dr Eleni Liapis (Department of Pathology, St Louis University Medical Center, St Louis, Mo.) and Professor O. K. Crosser (Chemical Engineering Department, University of Missouri-Rolla).

REFERENCES

1. M. Ebert and A. Howard, *Current Topics in Radiation Research*, Vol. 5. Elsevier, New York (1969).
2. J. I. Fabrikant, *Radiobiology*. Medical Publishers, Chicago, Ill. (1972).
3. E. J. Hall, *Radiobiology for the Radiologist* Harper & Row, New York (1978).
4. W. Mueller-Klieser, P. Vaupel and R. Manz, Tumor oxygenation under normobaric and hyperbaric conditions. *Br. J. Radiol.* **56**, 559–564 (1983).
5. J. Bergonie and Tribondeau, Interpretation of some results of radiotherapy and an attempt at determining a logical technique of treatment. *Radiat. Res.* **11**, 587–588 (1959).
6. H. M. Pratt, Quantitative aspects of radiation effects at the tissue and tumor level. *Am. J. Roentg.* **90**, 928 (1963).
7. P. Howard-Flanders and T. Alper, The sensitivity of microorganisms to irradiation under controlled gas conditions. *Radiat. Res.* **7**, 518–540 (1957).
8. M. M. Elkind, R. W. Swain, T. Alescio, H. Sutton and W. B. Moses, Oxygen, nitrogen, recovery and radiation therapy. In *Cellular Radiation Biology*, pp. 442–461. Williams & Wilkins, Baltimore, Md (1965).
9. L. H. Gray, Radiobiologic basis of oxygen as a modifying factor in radiation therapy. *Am. J. Roentg.* **85**, 803 (1961).
10. K. H. Clifton, R. L. Briggs and H. B. Stone, Quantitative radiosensitivity studies of solid carcinoma *in-vivo*: methodology and effect of anoxia. *J. natn. Cancer Inst.* **36**, 965 (1965).

11. R. S. Bush, R. D. T. Jenkins and W. E. C. Allt, Definitive evidence for hypoxic cells influencing care in cancer therapy. *Br. J. Cancer* **37**, 302–306 (1978).
12. I. Roizin-Towle and E. J. Hall, Studies with bleomycin and misonidazole on aerated and hypoxic cells. *Br. J. Cancer* **35**, 254–260 (1978).
13. W. L. Martin and N. J. McNally, The cytotoxic actions of adriamycin and cyclophosphamide on tumor cells *in-vitro* and *in-vivo*. *Int. J. Radiat. Oncol. Biol. Phys.* **5**, 1309 (1979).
14. E. Smith, I. J. Stratford and G. E. Adams, Cytotoxicity of adriamycin on aerobic and hypoxic Chinese hamster V79 cells *in-vitro*. *Br. J. Cancer* **41**, 568–573 (1980).
15. G. E. Adams, Hypoxia-mediated drugs for radiation and chemotherapy. *Cancer* **48**, 696 (1981).
16. I. Churchill-Davidson, *Frontiers of Radiation Therapy and Oncology*, Vol. 1 (Edited by I. M. Vaeth). Karger, Basel (1968).
17. R. A. Gatenby, L. R. Coia, M. P. Richter, H. Katz, P. J. Moldofsky, P. Engstrom, D. Q. Brown, R. Brookland and G. J. Broder, Oxygen tension in human tumors: *in-vivo* mapping using CT-guided probes. *Radiology* **156**, 211–214 (1985).
18. D. B. Carter and I. A. Silver, Quantitative measurements of oxygen tension in normal tissues and in tumors of patients before and after radiotherapy. *Acta radiol.* **53**, 233 (1960).
19. N. T. S. Evans and P. F. D. Naylor, The effect of oxygen breathing and radiotherapy upon the tissue oxygen tension of some human tumors. *Br. J. Radiol.* **36**, 418 (1963).
20. T. B. Constable and M. T. S. Evans, A method for measuring the spatial distribution of tissue oxygen removal rates. *Respir. Physiol.* **25**, 175–190 (1975).
21. K. A. Hultborn and A. Forssberg, Irradiation of skin tumors during pure oxygen inhalation. *Acta radiol.* **42**, 475 (1954).
22. I. Churchill-Davidson, C. Sanger and R. H. Thomlinson, High pressure oxygen and radiotherapy. *Lancet* **18**, 1091 (1955).
23. H. A. S. Van Den Brenk, J. P. Madigan and R. C. Kerr, *Clinical Application of Hyperbaric Oxygen*. Elsevier, Amsterdam (1964).
24. N. Milne, R. P. Hill and R. S. Bush, Factors affecting hypoxic KHT tumor cells in mice breathing O_2, $O_2 + CO_2$, or hyperbaric oxygen with or without anaesthesia. *Radiology* **106**, 663–671 (1973).
25. S. Dische, Hyperbaric oxygen Medical Research Council trials and their clinical significance. *Br. J. Radiool.* **51**, 888–894 (1978).
26. R. Johnson, Hyperbaric oxygen as a radiation sensitiser for carcinoma of the cervix. *Int. J. Radiat. Oncol. Biol. Phys.* **5**, 2151–2155 (1979).
27. W. T. Sause and H. P. Plenk, Radiation therapy of head and neck tumors: a randomised study of treatment in air versus treatment in hyperbaric oxygen. *Int. J. Radiat. Oncol. Biol. Phys.* **5**, 1833 (1979).
28. H. D. Suit, P. Maimonis, H. B. Michaelis and R. S. Sedlaek, Comparison of hyperbaric oxygen and misonidazole in fractionated irradiation of murine tumors. *Radiat. Res.* **87**, 360–367 (1981).
29. J. M. Brown, Evidence for acutely hypoxic cells in mouse tumors, and a possible mechanism of reoxygenation. *Br. J. Radiol.* **52**, 650–656 (1979).
30. J. D. Chapman, The detection and measurement of hypoxic cells in solid tumors. *Cancer* **54**, 2441–2449 (1984).
31. J. Crank and R. S. Gupta, A moving boundary problem arising from the diffusion of oxygen in absorbing tissue. *J. Inst. Math. Applic.* **10**, 19–33 (1972).
32. A. E. Berger, C. Melvyn and J. C. W. Rogers, Numerical solution of a diffusion consumption problem with a free boundary. *SIAM Jl numer. Analysis* **12**, 646–672 (1975).
33. D. L. S. McElwain and P. J. Ponzo, A model for the growth of a solid tumor with non-uniform oxygen consumption. *Mathl Biosci.* **35**, 267–279 (1977).
34. D. L. S. McElwain, A re-examination of oxygen diffusion in a spherical cell with Michaelis–Menten oxygen uptake kinetics. *J. theor. Biol.* **7**, 255–263 (1978).
35. I. A. Silver, M. Erecinska and H. I. Bicher, *Oxygen Transport to Tissue—III*. Plenum Press, New York (1978).
36. H. P. Greenspan, Models for the growth of a solid tumor by diffusion. *Stud. appl. Math.* **4**, 317–340 (1972).
37. E. A. Swabb, J. Wei and P. M. Gullino, Diffusion and convection in normal and neoplastic tissues. *Cancer Res.* **34**, 2814–2822 (1974).
38. A. S. Deakin, Model for the growth of a solid *in-vitro* tumor. *Growth* **39**, 159–165 (1975).
39. P. Vaupel and G. Thews, pO_2 distribution in tumor tissue of DS-carcinosarcoma. *Oncology* **30**, 475–484 (1974).
40. P. Vaupel, Hypoxia in neoplastic tissue. *Microvasc. Res.* **13**, 399–408 (1977).
41. P. Vaupel, Oxygen supply to malignant tumors. In *Tumor Blood Circulation* (Edited by H. I. Peterson), pp. 143–163. CRC Press, Boca Raton, Fla (1979).
42. J. Grote, R. Susskind and P. Vaupel, Oxygen diffusivity in tumor tissue (DS-carcinosarcoma) under temperature conditions within the range of 20–40°C. *Pflügers Arch. ges. Physiol.* **372**, 37–42 (1977).
43. D. F. Bruley and D. H. Hunt, Oxygen transport in tissue. *Microvasc. Res.* **8**, 314–319 (1974).
44. W. E. King, D. S. Schultz and R. A. Gatenby, Multi-region models for describing oxygen tension profiles in human tumors. *Chem. Engng Commun.* (in press).
45. A. I. Liapis, G. G. Lipscomb, O. K. Crosser and E. Tsiroyianni-Liapis, A model of oxygen diffusion in absorbing tissue. *Mathl Modelling* **3**, 83–92 (1982).
46. B. H. Arve, Oxygen absorption and diffusion in tissue. M.S. Thesis, Univ. of Missouri-Rolla, Mo. (1985).
47. J. R. Ockendon and W. R. Hodgkins, *Moving Boundary Problems in Heat Flow and Diffusion*. Clarendon Press, Oxford (1975).
48. S. B. Leite, M. N. Ozisik and K. V. Verghese, On the solution of linear diffusion problems in media with moving boundaries. *Nucl. Sci. Engng* **76**, 345–350 (1982).
49. T. Saitoh, Numerical method for multi-dimensional freezing problems in arbitrary domains. *Trans. ASME J. Heat Transfer* **100**, 294–299 (1978).
50. R. M. Furzerland, A comparative study of numerical methods for solving moving boundary problems. *J. Inst. Math. Applic.* **26**, 411–429 (1980).
51. V. Voller and M. Cross, Accurate solutions of moving boundary problems using the enthalpy method. *Int. J. Heat Mass Transfer* **24**, 545–556 (1981).
52. S. J. Khang and O. Levenspiel, The suitability of an *n*th-order rate form to represent deactivating catalyst pellets. *Ind. Engng Chem. Fundam.* **12**, 185–190 (1973).

53. J. Villadsen and M. L. Michelsen, *Solution of Differential Equation Models by Polynomial Approximation.* Prentice-Hall, Englewood Cliffs, N.J. (1978).
54. C. D. Holland and A. I. Liapis, *Computer Methods for Solving Dynamic Separation Problems.* McGraw-Hill, New York (1983).
55. L. H. Gray, A. D. Longer, M. Ebert, S. Hornsly and O. C. A. Scott, The concentration of oxygen dissolved in tissue at the time of irradiation as a factor in radiotherapy. *Br. J. Radiol.* **26**, 638–648 (1953).
56. E. E. Deschner and L. H. Gray, Influence of oxygen tension on X-ray-induced chromosomal damage in Ehrlich ascites tumor cells irradiated *in vitro* and *in vivo*. *Radiat. Res.* **11**, 115–146 (1959).
57. J. Breakwell and H. Chernoff, Sequential tests of the mean of a normal distribution, II: (Large t). *Ann. Math. Statist.* **35**, 162–173 (1964).
58. T. D. Wentzel, A free boundary problem for the heat equation. *Soviet Math.* **1**, 358–361 (1960).
59. W. Fulks and R. B. Guenther, A free boundary problem and an extension of Muskat's model. *Acta math.* **122**, 273–300 (1969).
60. A. E. Scheidegger, *The Physics of Flow Through Porous Media*, 2nd edn. Macmillan, New York (1960).
61. L. I. Rubinstein, *The Stefan Problem.* American Mathematical Society, Providence, R.I. (1971).
62. J. W. Enig, Approximate solutions in the theory of thermal explosions for semi-infinite explosives. *Proc. R. Soc. Ser. A* **305**, 205–217 (1968).